On-chip vacuum microtriode using carbon nanotube field emitters

C. Bower, W. Zhu,[a] D. Shalom, D. Lopez, L. H. Chen, P. L. Gammel, and S. Jin
Agere Systems Inc., 600 Mountain Avenue, Murray Hill, New Jersey 07974

(Received 20 February 2002; accepted for publication 4 April 2002)

We show a fully integrated, on-chip, vacuum microtriode fabricated via silicon micromachining processes using carbon nanotubes as field emitters. The triode is constructed laterally on a silicon surface using microelectromechanical systems (MEMS) design and fabrication principles. The technique incorporates high-performance nanomaterials in a MEMS design with mature solid-state fabrication technology to create miniaturized, on-chip power amplifying vacuum devices, which could have important and far-reaching scientific and technological implications. © *2002 American Institute of Physics.*
[DOI: 10.1063/1.1480884]

Microwave power tube amplifiers are compact and efficient for many high-power and high-frequency applications. They are the amplifier of choice for radar, electronic warfare, and space-based communications. The use of cold cathodes in vacuum devices further promises to bring together the best features of both vacuum tubes (e.g., high power) and solid-state power transistors (e.g., long lifetime and miniaturization). Cold cathode devices can be turned on instantaneously, without a tedious warm-up period. They can also be operated more efficiently because of the elimination of heating power and the possible incorporation of depressed collectors in the tube to recycle the kinetic energy of the electron beam back to the power supply. Further, in the absence of thermal distortions from the hot cathodes, the grid can now be placed very close to the cathode (e.g., $<10\ \mu$m), enabling high frequency (e.g., >10 GHz) and low control voltage (e.g., 50–100 V) operation.

Over the years, there have been considerable efforts spent in building cold cathode microwave power tube amplifiers.[1–13] All devices have been based on Spindt-type field emitter array (FEA) cathodes as the electron source. Traveling wave tubes operating at 10 GHz with molybdenum FEAs emitting at a current density of 50 A/cm^2 for a period of 5000 h (at 1% duty cycle) have been demonstrated.[11–13] However, density modulation at microwave frequencies through gated emission has proven to be difficult due to inadequate emission stability and reliability of the FEA cathodes. As a result, continuous operation of beam tube devices has not been possible, and no practically useful triodes have been reported.

Carbon nanotubes have recently emerged as promising field emitters that can emit large current densities at relatively low electric fields.[14] They are composed of cylindrically arranged graphitic sheets with diameters in the range of 1–30 nm and length/diameter aspect ratios greater than 1000.[15] Of particular interest is the capability of nanotube emitters to stably deliver very high emission currents, as individual nanotubes can emit up to 1 μA[16] and nanotube films can generate current densities in excess of 4 A/cm^2.[17]

We report here a method for fabricating fully integrated, on-chip, vacuum microtriodes using carbon nanotubes as field emitters via silicon micromachining processes. In contrast to the conventional vertical structures based on Spindt FEAs[6,7] or metal nanopillar cathodes[18] that involve multilayer deposition and precision alignment, our triodes are constructed laterally on a silicon surface using microelectromechanical systems (MEMS) design and fabrication principles. This approach offers greater flexibility in designing sophisticated microwave devices and circuitries, employs simpler, more reliable and more precise fabrication processes, and produces completely integrated structures.

Our microtriodes were fabricated using a three-layer polycrystalline silicon micromaching process on a silicon nitride coated silicon substrate.[19] The triode structure was chosen because, despite its simple device geometry, its characterization can be easily parameterized and its behavior can provide important insight into the design and performance of more sophisticated devices. The triode here is a micrometer-scale version of a conventional vacuum triode, consisting of a cathode, a grid, and an anode. As shown in Fig. 1(a), each electrode is made of a hinged polysilicon panel that can be rotated and locked into position, once the panel is released by etching away the oxide underneath. Well-aligned carbon nanotubes were selectively grown on the cathode region, as shown in Fig. 1(b), by first depositing a thin, nanotube-nucleating catalyst layer of iron (50 Å) through a shadow mask, and then growing the nanotubes in a microwave plasma of ammonia/acetylene mixture at 750 °C (for details of nanotube deposition, see Refs. 20 and 21). The structure was then assembled by rotating the electrode panels and locking them into the upright positions, as shown in Fig. 1(c). This assembly was done under a microscope using a mechanical microprobe. However, various self-assembly techniques could be used to achieve better manufacturability for future devices.[22] The carbon nanotubes grown here were multiwalled and highly oriented, with diameters ranging from 20–50 nm. The nanotube length was determined by controlling the growth time (typical growth rates were $\sim 10\ \mu$m in length per minute), which, in turn, controlled the spacing between the cathode and grid (and hence the emission field). Figure 2 shows a scanning electron microscopy

[a]Author to whom all correspondence should be addressed; Electronic mail: wzhu@agere.com

 © 2002 American Institute of Physics
Downloaded 24 Feb 2003 to 132.239.1.230. Redistribution subject to AIP license or copyright, see http://ojps.aip.org/aplo/aplcr.jsp

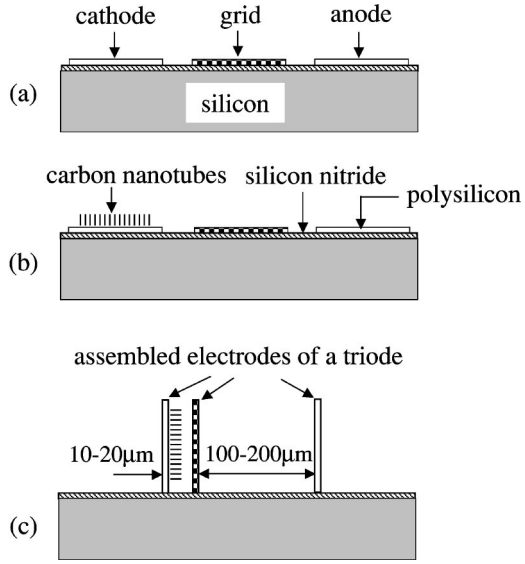

FIG. 1. A flow diagram illustrating the fabrication procedure of our microtriode. (a) Polysilicon electrode panels are etched and released on a silicon nitride coated Si substrate (etched oxide regions are not shown), (b) carbon nanotubes are selectively grown on the cathode, and (c) the electrodes panels are rotated and locked into their upright positions to constitute a laterally built triode.

(SEM) micrograph of a completely assembled microtriode, with the inset showing the structural details of the cathode and grid regions. The nanotubes are seen as a blank patch on the cathode about $50\times50\ \mu m^2$ in area and 10 μm in length, leaving a 10 μm spacing between the cathode and the grid.

We have obtained the dc characteristics of the triode by measuring how the anode current (I_a) changes as a function of both the grid voltage (V_g) and the anode voltage (V_a). Figure 3 presents the grid current (I_g), anode current (I_a), and transconductance ($g_m=\delta I_a/\delta V_g$) varying with the grid voltage while the anode voltage was held at 100 V. We observed that the grid and anode currents increased exponentially with the grid voltage, as was expected from the Fowler–Nordheim emission tunneling theory.[23] Under reverse bias conditions, no current was observed until electric breakdown of the insulating silicon nitride layer occurred at approximately 130 V. The Fowler–Nordheim plot, shown in

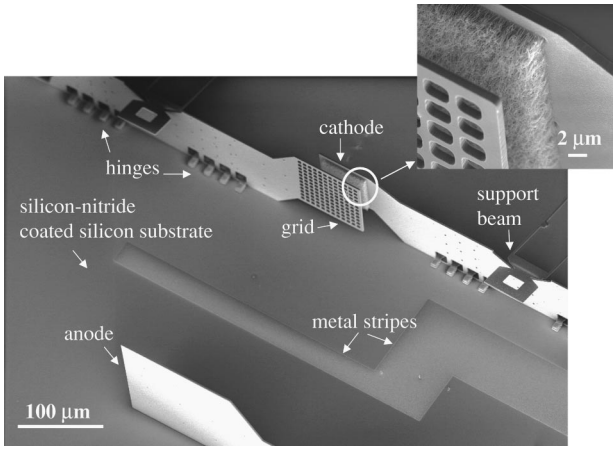

FIG. 2. An SEM micrograph of a completely assembled microtriode. The bond pads for electrical contact are not shown. The metal strips lying on the substrate surface between the grid and anode are for charge reduction if electrons hit the surface.

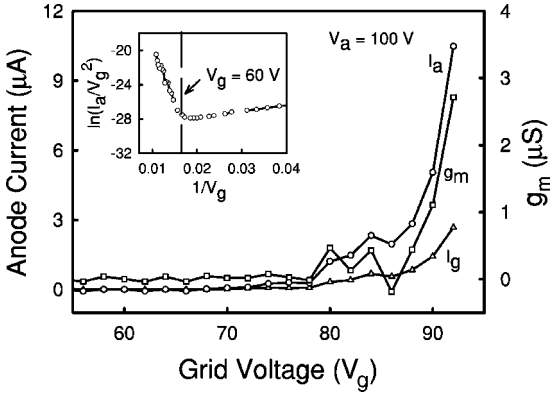

FIG. 3. (a) Grid current, anode current, and transconductance as functions of grid voltage with the anode held at 100 V. The inset is a Fowler–Nordheim plot showing that the emission occurred at the grid voltage of 60 V, corresponding to an onset field of 6 V/μm.

the inset in Fig. 3, indicates that the grid voltage required for electron emission from the nanotube emitters was 60 V, corresponding to an onset field of 6 V/μm. The anode and grid currents were observed to follow each other closely, with a current ratio (I_a/I_g) of roughly 4 for this particular device tested. This ratio is expected to improve significantly if the nanotubes were grown patterned on the cathode according to the grid geometry instead of the blank layer here. The total emission current (I_g+I_a) from this device was 13.3 μA which corresponded to a macroscopic emission current density of roughly 0.5 A/cm^2 from the cathode.

The transconductance of this triode was 2.7 μS at the anode current of 10.6 μA. It should be correspondingly much higher if the total emission current can be increased. On a normalized basis with respect to the cathode area, our number (0.11 S/cm^2 at $I_a=10.6\ \mu$A) is less than half of that from the thermionic triode (0.3 S/cm^2),[24] but can be improved at higher current levels. If normalized by the emission current, our number (0.25 S/A) is significantly better than Spindt cathode-based structures ($\sim$0.03 S/A). While it is important to have a high transconductance for successful high-frequency device operation, such a high transconductance is desirably achieved at relatively low emission currents and voltages in order to reduce the probability of emitter failure due to overheating or arcing and to minimize the heat dissipation at the anode. Because the fields required for emission from nanotubes are low, our nanotube based triode structure is likely to perform well in this regard.

Figure 4 shows the measured anode characteristic curves. As noted earlier, electric breakdown occurred across the thin silicon nitride layer on the Si substrate at voltages above 130 V. As a result, data were collected only at anode voltages below 100 V, above which excessive leakage current through the substrate rendered meaningful current measurements difficult. The internal anode resistance ($R_a=\delta V_a/\delta I_a$) was approximately 10 M$\Omega$ at $V_g=92$ V but could be much higher if operating at the current saturation regions (45 MΩ at $V_g=86$ V and 65 MΩ at $V_g=80$ V). As illustrated by the 10 MΩ load line and assuming that the device was operated at $V_a=60$ V and $I_a=4\ \mu$A, a peak-to-peak voltage swing of 6V on the grid would induce a peak-to-peak anode voltage change of 40 V, resulting in a voltage gain of 16.5 dB. Assuming that the load resistance (R_l) is

Downloaded 24 Feb 2003 to 132.239.1.230. Redistribution subject to AIP license or copyright, see http://ojps.aip.org/aplo/aplcr.jsp

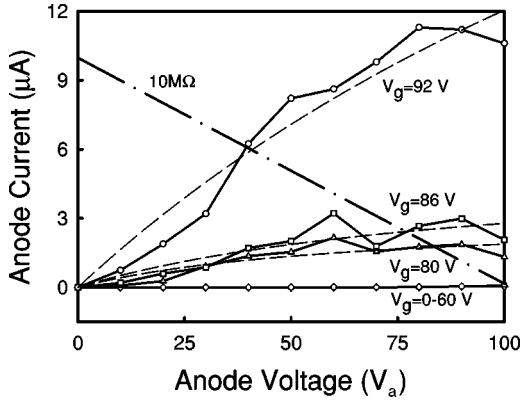

FIG. 4. Anode current as a function of anode voltage at various grid voltages. The dashed lines are fits to the data. The 10 MΩ load line is used to illustrate the voltage gain that can be achieved by this device.

equal to the internal anode resistance (R_a), we can conveniently compare the output power delivered at the anode (P_a) with the power lost at the gird (P_g) as $P_a/P_g = \frac{1}{4}\ (I_a{}^2R_l)/(I_gV_g) = \frac{1}{4}(I_a/I_g)g_mR_a$. Using a current ratio (I_a/I_g) of 4, a transconductance (g_m) of 2.7 μS, and an anode (and load) resistance (R_a and R_l) of 10 MΩ, we obtain $P_a/P_g = 27$, indicating that the dc output power is 27 fold more than the power lost (or intercepted) at the grid. Because of the breakdown of the silicon nitride layer, the total output power at the integrated anode is currently limited at about 1 mW, corresponding to an output power density of 10 W/cm^2 of anode area. Assuming that these devices will eventually be built on a better substrate with a much larger breakdown voltage, we expect that an output power of 100 mW (100 μA at 1000 V) per device is obtainable. In a distributed amplifier system,[4] this would require only 100 devices to generate 10 W of power.

Based on the results of the dc measurements, it is possible to discuss the potential frequency performance of this device. Because the current structure is primarily designed to test the feasibility of the MEMS device concept, not for high-frequency operation, the actual frequency performance is currently dominated by stray capacitance and lead inductance. In theory, the cutoff frequency of a triode depends critically on the transconductance and the interelectrode capacitance ($f_t = g_m/2\pi C_g$). For the microtriode, the cathode-to-grid capacitance can be roughly approximated using parallel-plate geometry. Using a cathode area of (50×50) μm^2 and a cathode-to-grid distance of 10 μm, the capacitance ($C = \varepsilon_o(A/d)$) can be calculated to be 2.2×10^{-3} pF. Using this C_g and a transconductance of 2.7 μS, we derive the cutoff frequency to be 195 MHz.

In summary, we have demonstrated a completely integrated, laterally built, on-chip microtriode that incorporates carbon nanotube field emitters and provides dc output power. The design allows multiple devices to be integrated on a single chip, which can be used to form a part of complex microwave circuits to meet various power amplification needs. We are encouraged by the fact that the MEMS structure and materials withstood the high-temperature nanotube growth processing and the resulting device still demonstrated impressive dc power characteristics. Based on the dc data already obtained, we will perform rf modeling and design optimization on both the device and circuit levels and further explore device structures that are more compatible with high-frequency operation. With the use of better breakdown-resistant substrates and improved electrode designs, we expect to achieve transconductances of at least 100 μS per device, which would increase the output power and cutoff frequency by two orders of magnitude. We will take advantage of the MEMS design flexibility to add more functionality into the device structure. More importantly, the powerful combination of nanomaterials with MEMS technology, as demonstrated in this work, will likely stimulate further advances in creating new and unique devices useful for a variety of applications.

The authors would like to acknowledge the partial financial support from the Office of Naval Research for this project.

[1] F. M. Charbonnier, J. P. Barbour, L. F. Garrett, and W. P. Dyke, Proc. IEEE 991 (1963).
[2] I. Brodie and C. A. Spindt, Appl. Surf. Sci. **2**, 149 (1979).
[3] P. M. Lally, Y. Goren, and E. A. Nettesheim, IEEE Trans. Electron Devices **36**, 2738 (1989).
[4] H. G. Kosmahl, IEEE Trans. Electron Devices **36**, 2728 (1989).
[5] W. Friz and M. Ettenberg, in Proceedings of the Third International Conference on Vacuum Microelectronics, Monterey, CA, 1990.
[6] R. E. Neidert, P. M. Phillips, S. T. Smith, and C. A. Spindt, IEEE Trans. Electron Devices **38**, 661 (1991).
[7] C. E. Holland, A. Rosengreen, and C. A. Spindt, IEEE Trans. Electron Devices **38**, 2368 (1991).
[8] J. P. Calame, H. F. Gray, and J. L. Shaw, J. Appl. Phys. **73**, 1485 (1993).
[9] C. A. Spindt, C. E. Holland, A. Rosengreen, and I. Brodie, J. Vac. Sci. Technol. B **11**, 468 (1993).
[10] P. M. Phillips, R. E. Neidert, L. Malsawma, and C. Hor, IEEE Trans. Electron Devices **42**, 1674 (1995).
[11] H. Makishima, H. Imura, M. Takahashi, H. Fukui, and A. Okamoto, Proceedings of the Tenth International Conference on Vacuum Microelectronics, Kyongju, Korea (1997), p. 194.
[12] H. Takemura, Y. Yomihari, N. Furutake, F. Matsuno, M. Yoshiki, N. Takada, A. Okamoto, and S. Miyano, Tech. Dig. Int. Electron Devices Meet. 709 (1997).
[13] H. Imura, S. Tsuida, M. Takahasi, A. Okamoto, H. Makishima, and S. Miyano, Tech. Dig. Int. Electron Devices Meet. 721 (1997).
[14] W. Zhu, P. K. Baumann, and C. A. Bower, in *Vacuum Microelectronics*, edited by W. Zhu (Wiley, New York, 2001), Chap. 6, p. 247.
[15] S. Ijima, Nature (London) **354**, 56 (1991).
[16] K. A. Dean and B. R. Chalamala, Appl. Phys. Lett. **76**, 375 (2000).
[17] W. Zhu, C. Bower, O. Zhou, G. Kochanski, and S. Jin, Appl. Phys. Lett. **75**, 873 (1999).
[18] A. A. G. Driskill-Smith, D. G. Hasko, and H. Ahmed, Appl. Phys. Lett. **75**, 2845 (1999).
[19] http://www.memsrus.com: The Design Handbook of MUMPs (Multi-User MEMS Processes), Cronos Integrated Microsystems, a JDSU Company, Research Triangle Park, North Carolina, 2000.
[20] C. Bower, W. Zhu, S. Jin, and O. Zhou, Appl. Phys. Lett. **77**, 830 (2000).
[21] C. Bower, W. Zhu, D. J. Werder, S. Jin, and O. Zhou, Appl. Phys. Lett. **77**, 2767 (2000).
[22] G. T. A. Kovacs, *Micromachined Transducers Sourcebook* (McGraw–Hill, Boston, 1998).
[23] R. H. Fowler and L. Nordheim, Proc. R. Soc. London, Ser. A **119**, 173 (1928).
[24] J. A. Morton and R. M. Ryder, Bell Syst. Tech. J. **29**, 496 (1950).

Downloaded 24 Feb 2003 to 132.239.1.230. Redistribution subject to AIP license or copyright, see http://ojps.aip.org/aplo/aplcr.jsp